

Unveiling Dark Matter with HI and H α Data - Observational Problems

G. Gentile¹, D. Vergani¹, P. Salucci², P. Kalberla¹, U. Klein¹

¹Radioastronomisches Institut Univ. Bonn, Auf dem Hugel 71, D-53121 Bonn, Germany

²SISSA, via Beirut 4, I-34013 Trieste, Italy

Abstract

We present combined H α +HI rotation curves for a sample of spiral galaxies. Most of the velocity profiles (spectra at single points) in these galaxies are asymmetric, preventing the use of standard methods like the first moment analysis and the single Gaussian fitting. We thus propose a method similar to the Envelope-Tracing method (Sofue & Rubin 2001) to analyse those profiles from which we obtain HI rotation curves in good agreement with the H α rotation curves. These final rotation curves provide the required high resolution in the inner parts of the galaxies, but also extend out to typically 2-3 R_{opt} . They will hence allow us to investigate the distribution of dark matter.

1 Introduction

The study of rotation curves of spiral galaxies provides the best evidence for dark matter on galactic scales. However, important properties like the shape of the dark halo, the distribution of dark matter and the relative importance of dark and luminous matter are still questions under debate. Recent results from the analysis of rotation curves (Borriello & Salucci 2001 for normal spirals, de Blok et al. 2002 for low surface brightness galaxies) seem to favour dark halos with constant density cores. However the debate is still going on as to whether the available data have sufficient quality to constrain the distribution of dark matter (Primack 2002). For this reason high-quality data with high resolution and large spatial extension are needed. This can be ideally achieved by combining H α rotation curves (for the high resolution) and HI rotation curves (for the extension to large galactocentric radii). In particular, the high resolution in the inner parts is crucial to deduce the shape of the density profile (Blais-Ouellette et al. 2001), while the extension to large radii is needed to constrain the size of the possible core (Borriello & Salucci 2001). All these considerations can be done for the local Universe; the Atacama Large Millimeter Array (ALMA) will enable us to investigate the structure and evolution of dark matter halos at high redshifts.

2 Observations

Our galaxies were selected from the high-quality subsample of H α rotation curves presented in Persic & Salucci (1995), by finding a compromise between the following criteria: high angular extent (to maximise θ_{beam}/R_d , see Table 1), low luminosity (so that the radius where dark matter starts to dominate the kinematics is smaller, see Salucci & Persic 1999), high HI flux (to have better

Galaxy	M_I	R_d (")	θ_{beam} (")
ESO 116-G12	-20.0	22.7	30.4 x 24.4
ESO 121-G6	-20.4	24.4	32.2 x 22.7
ESO 123-G23	-20.8	13.2	30.6 x 25.0
ESO 240-G11	-22.3	26.3	33.8 x 25.6
ESO 269-G19	-22.3	25.4	34.3 x 22.0
ESO 287-G13	-21.7	26.3	32.6 x 24.6
ESO 79-G14	-21.4	19.0	27.4 x 23.0
NGC 1090	-21.8	19.3	17.6 x 14.7
NGC 7339	-20.6	17.9	13.9 x 13.5

Table 1: The sample: M_I is the absolute magnitude in the I-band, R_d is the exponential scale-length of the stellar disk and θ_{beam} is the size of the radio beam

S/N in the HI data) and symmetry of the $H\alpha$ rotation curve (to minimise the effect of non-circular motions). Our sample currently consists of nine galaxies, and we expect to enlarge it in the future.

For the observation and reduction of the optical data ($H\alpha$ spectroscopy and I-band photometry) we refer to Persic & Salucci (1995) and Mathewson, Ford & Buchhorn (1992).

The HI observations of NGC 1090 and NGC 7339 were performed with the VLA in the C-array, while the other galaxies were observed with the ATCA in the 750m and 1.5km configurations.

3 Data analysis

The standard reduction and analysis was performed with the software packages AIPS, *miriad* and GIPSY. In Table 1 we list some properties of the galaxies of our sample. NGC 1090 is the only galaxy of the sample that permits sufficient sampling of the velocity field to allow the use of the tilted ring modelling (Begeman 1989). In all other cases the combination of high inclination and a large beam (compared with the size of the galaxy) prevents us from using this method. We therefore traced the rotation curve along the warp on points defined like in García-Ruiz (2001) and implemented for kinematical use by Vergani et al. (2002).

In all the cases - the galaxy suited for tilted ring modelling and the other galaxies - we derived the rotation curves by analysing the velocity profiles (spectra at single points). In Figure 1 we show an example of a typical profile at an intermediate galactocentric distance: the profile is not symmetrical and it has a tail towards the systemic velocity. This is what we expect in the case of a highly inclined galaxy, because (see Fig. 2) what we observe is the integration along a large portion of the disk, so that also material with lower radial velocities contributes to the velocity profile.

Moreover, from recent results (Swaters et al. 1997, Fraternali et al. 2002), it seems that at least in a few spiral galaxies there is some neutral hydrogen at several kpc from the galactic plane that rotates more slowly than the gas in the disk; this effect produces an asymmetry of the velocity profiles (a “beard” in the position-velocity diagram, Fraternali et al. 2002) also in galaxies that do not have a high inclination.

The result is that the standard methods of first moment (intensity weighted mean) and single Gaussian fitting provide velocities that are biased towards the systemic velocity (see Fig. 1) and cannot be used to determine the rotation velocity.

4 The Modified Envelope-Tracing method

We thus applied a method similar to the Envelope-Tracing method (e.g. Sofue & Rubin 2001), in order to fit only the side of the profiles that we are interested in, the extreme velocity side. We call it *Modified Envelope-Tracing* (MET) method when applied to the whole velocity field and *WArped Modified Envelope-Tracing* (WAMET) method when applied only on the ridge of the possible warp:

- we first fitted a half-Gaussian from the peak value to the extreme velocity side of the profiles and we considered the velocity at half maximum (v_t)
- then the rotation velocity is given by the following equation:

$$v_{\text{rot}} = |v_t - v_{\text{sys}}| / \sin i - \sqrt{(0.5 \cdot \text{FWHM}_{\text{ISM}})^2 + (0.5 \cdot \text{FWHM}_{\text{instr}})^2 + (0.5 \cdot \text{FWHM}_{\text{beam}})^2} \quad (1)$$

where i is the inclination, and the terms indicated as FWHM describe the effects that we assume are broadening our profiles:

- FWHM_{ISM} is the broadening due to the turbulence of the interstellar medium; consistently with Kamphuis (1993) we consider a $\sigma_{\text{ISM}} = \text{FWHM}_{\text{ISM}} / \sqrt{8 \ln 2}$ going from 12 km/s in the inner parts to 7 km/s in the outer parts of the galaxy.
- $\text{FWHM}_{\text{instr}}$ is the instrumental contribution, that we take equal to the channel resolution
- $\text{FWHM}_{\text{beam}}$ is a rough estimate of the broadening of the profiles due to the beam: as it is evident in Fig. 3, a larger beam will sample a larger portion of the velocity field and will thus broaden the profiles, even on their extreme velocity side.

According to Sancisi & Allen (1979) an upper limit to v_{rot} can be given by setting $\text{FWHM}_{\text{beam}} = 0$.

To estimate a lower limit to v_{rot} , in a way similar to Braun (1997) we consider that the error due to the beam that we make in measuring the width of the profiles is given by: $2 \cdot (v(r \pm \theta_{\text{beam}}/2) - v(r))$

where the positive sign applies when the gradient of the velocity field is positive and the negative sign when it is negative.

Remembering that we have an upper and a lower limit to v_{rot} , we decided to take the middle point, i.e. we considered the following correction:

$$\text{FWHM}_{\text{beam}} = v(r \pm \theta_{\text{beam}}/2) - v(r)$$

We preferred to use this method instead of others for numerous reasons:

- The profiles are asymmetric, thus methods assuming symmetry cannot be used to derive the rotation velocity
- We are interested only in the extreme velocity side of the profiles, which is not affected by projection effects
- This method accounts for a more realistically varying σ_{ISM} with radius, instead of keeping it fixed
- It also estimates the correction for the broadening of the profiles due to the beam, which can be substantial in regions where the gradient of the velocity field is high
- The WAMET method, applied to galaxies where the sampling of the velocity field is poor, enables us to trace the rotation curve along the possible warp instead of keeping a fixed position angle, like in methods based on the analysis of the position-velocity diagram; the shortcomings of keeping a fixed position angle are discussed in Vergani et al. (2002)

5 Rotation curves

In order to derive the rotation curves, we applied the tilted ring modelling to NGC 1090, while for the other galaxies we calculated the kinematical centre and the systemic velocity by minimising the differences between the two sides. The errors are the maximum between three values: the difference between the approaching and the receding side, our correction for the broadening of the profiles due to the beam, and a “minimum error” equal to $(2/\sin i)$ km/s.

In Fig. 3 we show the H α and HI rotation curves projected onto the HI position-velocity diagrams for 4 galaxies of our sample: the agreement between the two datasets is good and, as we should expect, the HI rotation curves follow the shape of the last contours of the position-velocity diagrams. We also show in Fig. 4 the H α and the HI rotation curves derived from three different methods: our (Warped) Modified Envelope-Tracing method, the first moment and the single-Gaussian fitting. The two latter methods yield a much worse agreement with the H α rotation curves, especially in the inner parts where the profiles are most asymmetric: in these cases the rotation velocities are severely underestimated.

From the combined H α +HI rotation curves we will be able to perform the mass decompositions with different models of the dark halos and to put constraints on the distribution of dark matter in our sample of spiral galaxies. As a further step, we plan to supplement and strengthen the method by employing high-resolution CO observations.

Acknowledgements

GG is grateful for financial support of the *Deutsche Forschungsgemeinschaft* under number GRK 118 “The Magellanic System, Galaxy Interaction and the Evolution of Dwarf Galaxies”. We thank the Observatoire de Bordeaux for the warm hospitality during the workshop.

References

- Begeman, K.G.: 1989, A&A 223, 47
Blais-Ouellette, S., Amram, P., Carignan, C.: 2001, AJ 121, 1952
Borriello, A., Salucci, P.: 2001, MNRAS 323, 285
Braun, R.: 1997, ApJ 484, 637
de Blok, W.J.G., McGaugh, S.S., Rubin, V.C.: 2001, AJ 122, 2396
Fraternali, F., van Moorsel, G., Sancisi, R., Oosterloo, T.: 2002, AJ 123, 3124
García-Ruiz, I.: 2001, Ph.D. thesis, Univ, Groningen
Kamphuis, J.: 1993, Ph.D. thesis, Univ, Groningen
Mathewson, D.S., Ford, V.L., Buchhorn, M.: 1992, ApJS 81, 413
Persic, M., Salucci, P.: 1995, ApJS 99, 501
Primack, J.R.: astro-ph/0205391
Salucci, P., Persic, M.: 1999, MNRAS 309, 923
Sancisi, R., Allen, R.J.: 1979, A&A 74, 73
Sofue, Y., Rubin, V.: 2001, Ann. Rev. Astron. Astrophys. 39, 137
Swaters, R.A., Sancisi, R., van der Hulst J.M.: 1997, ApJ 491, 140
Vergani, D., Gentile, G., Dettmar, R.-J., Aronica, G., Klein, U.: 2002, astro-ph/0206481, ALMA Extragalactic and Cosmology Science Workshop on Dark Matter, Bordeaux, http://www.observ.u-bordeaux.fr/public/alma_workshop/darkmatter/

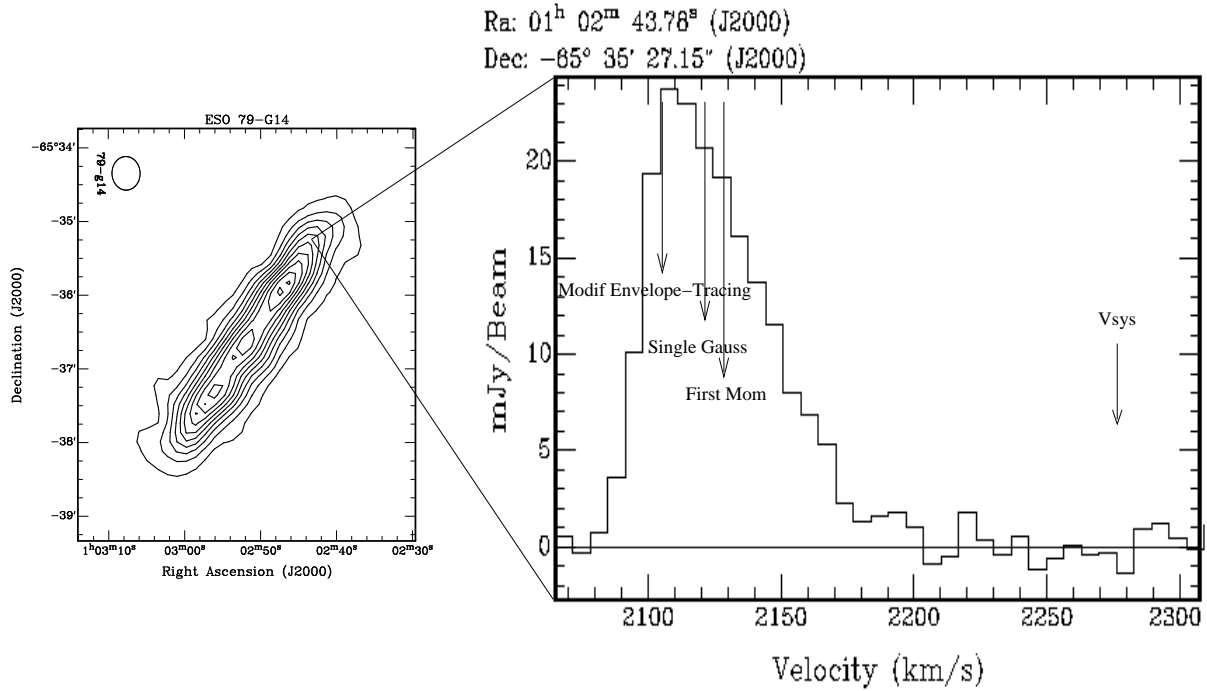


Figure 1: A typical spectrum of the galaxy ESO 79-G14 at an intermediate galactocentric distance. The arrows indicate the systemic velocity and the positions of the velocities derived from the first moment, from fitting a single Gaussian and from our Modified Envelope-Tracing Method

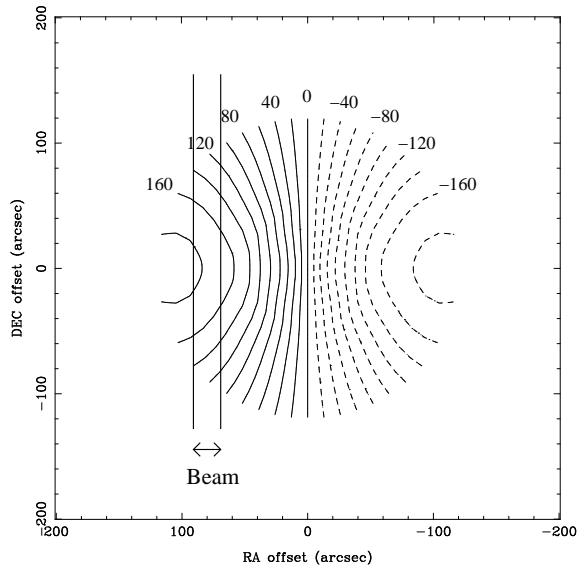


Figure 2: Model of the radial velocities in the plane of the galaxy ESO 79-G14

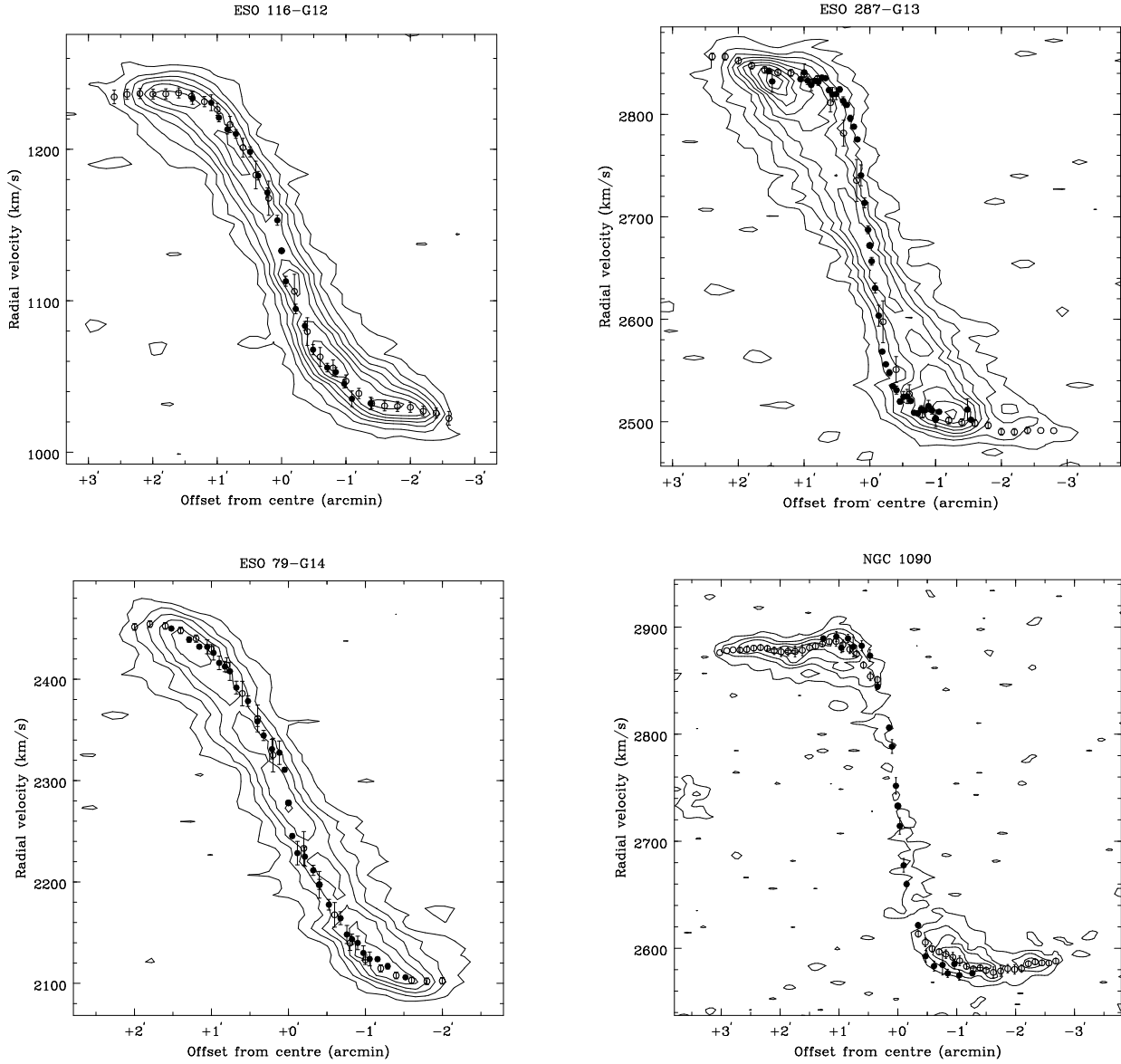


Figure 3: $H\alpha$ (filled circles) and HI rotation curves (empty circles) projected onto the HI position-velocity diagrams of 4 galaxies of our sample. We projected separately the two sides of the HI rotation curves. Since the difference between the two sides enters in our derivation of the error (see text), at the radii where only one side is present we did not define the error. The contours are $(2, 6, 10, \dots) \times \sigma$, with $\sigma=1.2$ mJy/beam for ESO 116-G12, ESO 287-G13 and ESO 79-G14 and $\sigma=0.8$ mJy/beam for NGC 1090

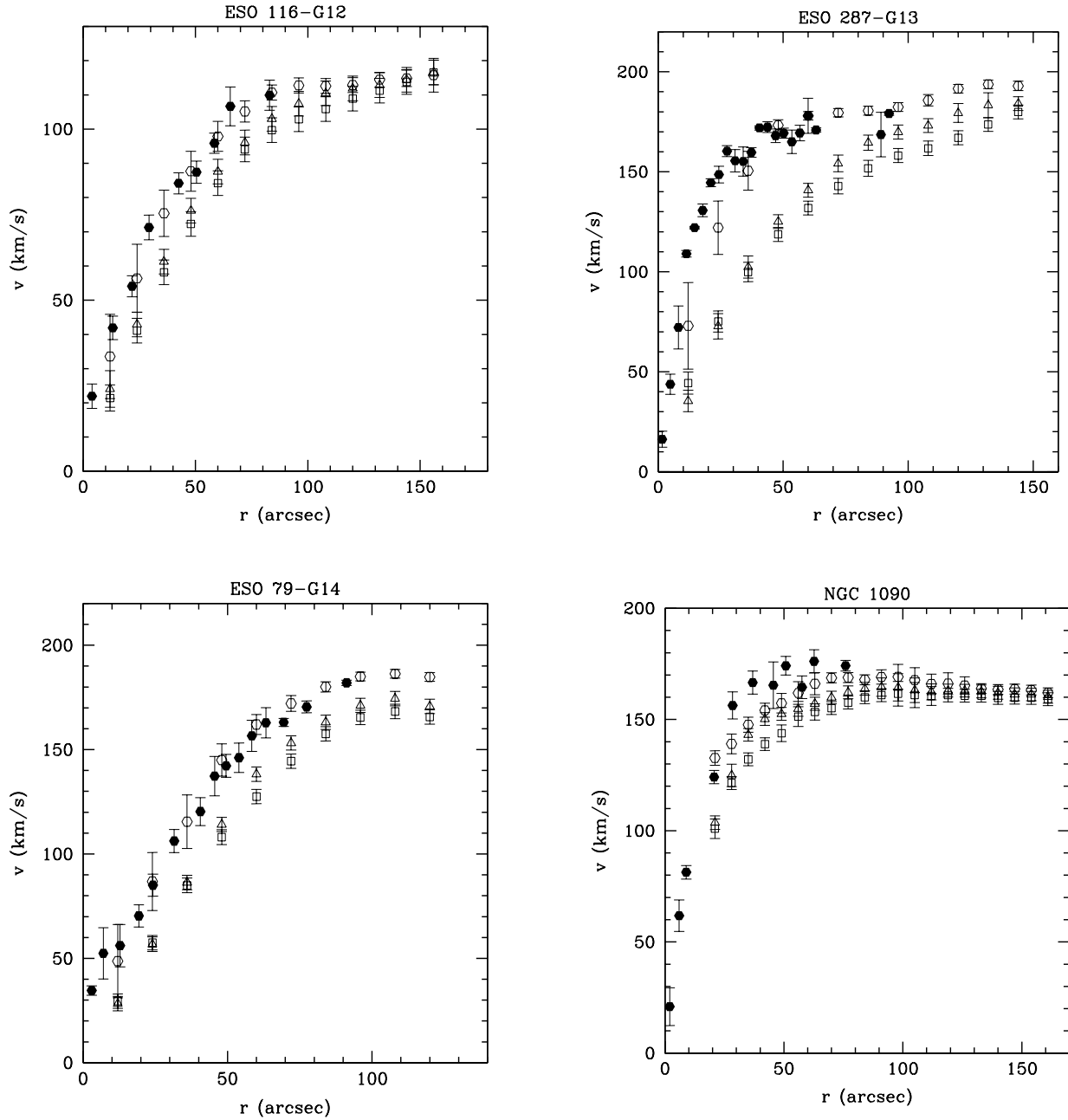


Figure 4: $H\alpha$ (filled circles) and HI rotation curves of the galaxies of Fig. 3 derived with different methods: our modified method (empty circles), the first moment (empty squares) and single-Gaussian fitting (empty triangles)